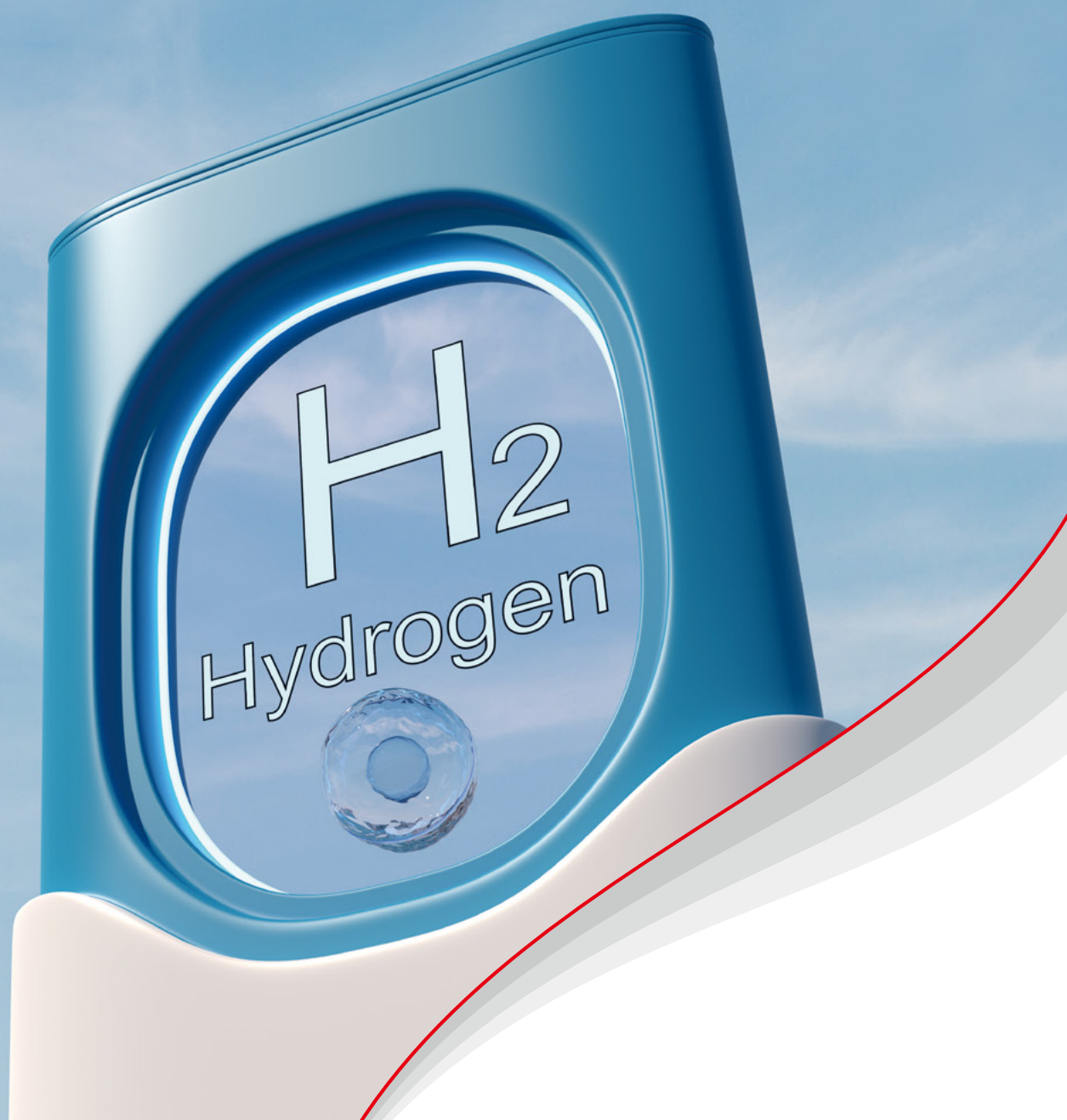


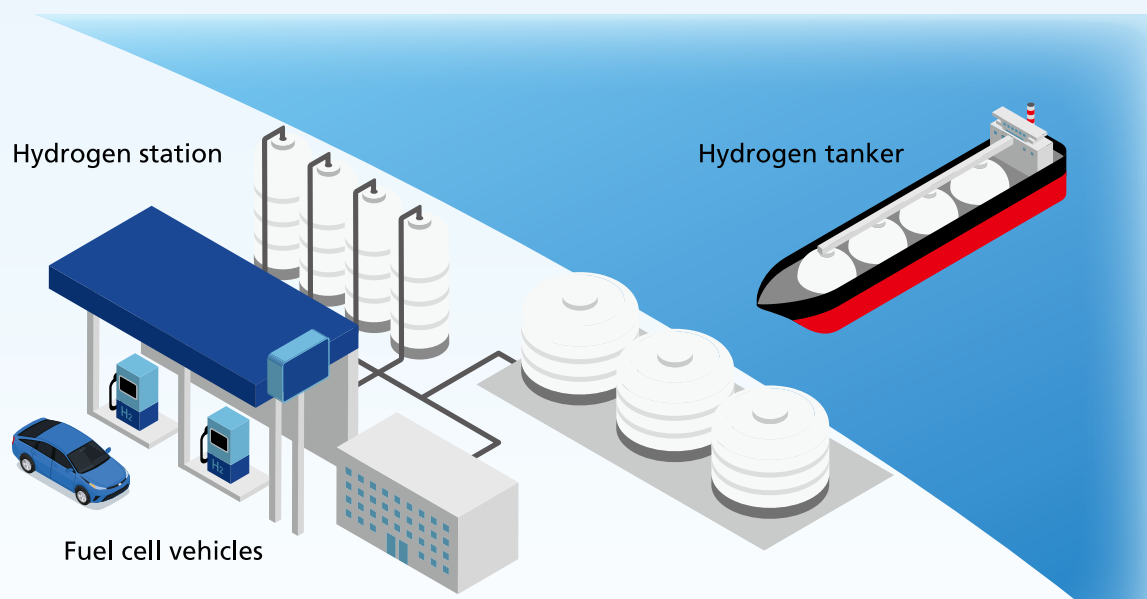
Analysis Solutions for

Quality Control of Hydrogen



The Coming Hydrogen Energy Society

Fuel cells for domestic use and fuel cell vehicles (FCV) are gradually becoming more common. Fuel cells produce electricity from hydrogen and are indispensable when it comes to realizing a hydrogen energy society. Hydrogen can be produced by various industrial processes, and its conversion with electrical power is easy. Therefore, its use as a fuel for thermal electrical power generation and for storage of natural energy, such as solar and wind, is being evaluated as the hydrogen energy society comes into focus.




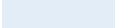
| Topics | Title | Products | Page |
|---|--|--|------|
| Measurement of Impurities in Hydrogen Gas | Trace Impurity Analysis of Hydrogen Fuel in Fuel Cell Vehicle-Related Fields | Gas Chromatograph | 5 |
| | Analysis of Inorganic Gases and Hydrocarbons by GC-MS | Gas Chromatograph Mass Spectrometer | 6 |
| | High-Resolution Analysis of Carbon Monoxide (CO) | Fourier Transform Infrared Spectrophotometer | 7 |
| Hydrogen Carrier | TOC Evaluation of Ammonia Solution | Total Organic Carbon Analyzer | 8 |
| | High-Sensitivity Analysis of Ammonia in Water | | 9 |
| | Analysis of Hydrogen in Solution | Gas Chromatograph | 10 |
| | Analysis of Hydrogen in Gas | | |
| Hydrogen Embrittlement | Analysis of Toluene, Methylcyclohexane (MCH) in Solution | Gas Chromatograph Mass Spectrometer | 11 |
| | Observation of Corroded Copper Pipe with a Microfocus X-ray CT System | Microfocus X-ray CT System | 12 |
| | Accurate Measurements of Micro-Displacements in a Compression Fatigue Test of a Gasket | Fatigue and Endurance Testing Machine | 13 |
| Catalytic Analysis | Quantitative Analysis of the Amount of Deposition and Plating Thickness: Multilayer and Irregular Shaped Samples | Energy Dispersive X-Ray Fluorescence Spectrometer | 14 |
| | Evaluation of a Catalyst Used in the Production of Fuel Cell Hydrogen | Transportable Gas Analyzer | 15 |
| | Analysis of an Automotive Three-Way Catalyst | Electron Probe Microanalyzer | 16 |
| | Analysis of an MEA (Membrane/Electrode Assembly) by EPMA | | 17 |
| Hydrogen Tank | Analysis of an MEA (Membrane/Electrode Assembly) by XPS | X-Ray Photoelectron Spectrometer | 18 |
| | Observation of Carbon Fiber Reinforced Thermoplastic Resin with an X-ray CT system | Microfocus X-ray CT System | 19 |
| | Verification and Validation of Uniaxial Tensile Test Simulation Results of Composites | Microfocus X-ray CT System Precision Universal Tester | 20 |
| | Example of Non-Destructive Inspection Using an Ultrasonic Optical Flaw Detector | Ultrasonic Optical Flaw Detector | 21 |
| | Measurement of Expansion Coefficient of Polymer Materials Using TMA | Thermomechanical Analyzer | 22 |
| | DCB Tests of CFRP | Precision Universal Tester | 23 |

Analysis of Impurities in Hydrogen

Impurities in hydrogen production affect subsequent industrial processes. Consequently, strict purity standards have been defined for hydrogen used in fuel cells (ISO 14687-2019). This is because if hydrogen contains carbon monoxide, sulfur components, etc., the catalyst of the fuel cell will be damaged. The hydrogen fuel standard for FCVs (ISO 14687 Type II Grade D) defines many items to be controlled, and Shimadzu analytical instruments can play a role in analyzing these items.

| ISO 14687 Grade D ($\mu\text{mol/mol}$) (ppm) | | System GC | GC-MS | GC | | | | IC | HPLC | FTIR |
|--|-------|--------------|-------|-----|-----|-----|-----|----|------|------|
| | | | | BID | TCD | FID | SCD | | | |
| H ₂ O | 5 | | | | | | | | | |
| Total Hydrocarbons (except CH ₄) | 2 | | | | | | | | | |
| CH ₄ | 100 | | | | | | | | | |
| O ₂ | 5 | | | | | | | | | |
| He | 300 | | | | | | | | | |
| N ₂ | 300 | | | | | | | | | |
| Ar | 300 | | | | | | | | | |
| CO ₂ | 2 | | | | | * | | | | |
| CO | 0.2 | | | | | * | | | | |
| Formaldehyde | 0.2 | | | | | | | | | |
| Formic acid | 0.2 | | | | | | | | | |
| Total sulfur compounds | 0.004 | | | | | | | | | |
| Halogen compounds | 0.05 | | | | | | | | | |
| Ammonia | 0.1 | | | | | | | | | |

 ISO14687-2019 compliant

 Less than ISO 14687-2019 standard but measurable

* Methanizer is needed.



Hydrogen Energy Analysis Solutions
for Quality Control of Hydrogen

Hydrogen Carrier

Hydrogen is difficult to store and transport long distances efficiently when left as a gas. A hydrogen carrier is an efficient way of storing and transporting hydrogen in the form of a liquid or a hydrogenated compound. Methods include liquefying the hydrogen or increasing the density of the compressed hydrogen gas. Another method involves converting the hydrogen into another substance that has a high hydrogen density and is more easily handled (such as organic hydrides, ammonia, or formic acid) and then removing the hydrogen from this substance for use. Rather than removing the hydrogen for use, the hydrogen energy can also be utilized by burning something like ammonia as is.

| | Pressurized Hydrogen (700 MPa) | Liquid Hydrogen | Organic Hydride (Methyl Cyclohexane) | Ammonia | Formic acid |
|---|-----------------------------------|-----------------|---|---------|-----------------|
| Molecular Weight | 2.0 | 2.0 | 98.2 | 17.0 | 46.0 |
| H ₂ Content (wt %) | 100.0 | 100.0 | 6.2 | 17.8 | 4.3 |
| Volumetric H ₂ Density (Kg-H ₂ /m ³) | 39.6 | 70.8 | 47.3 | 121 | 53 |
| Boiling Point (°C) | = | -253 | 101 | -33 | 101 |
| H ₂ Release Enthalpy Change* (kJ/mol-H ₂) | = | 0.9 | 67.5 | 30.6 | 31 (ΔG 4aq.) |

*H₂ release enthalpy change: Energy required to remove hydrogen

SIP Energy Carriers: https://www.jst.go.jp/sip/pdf/SIP_energycarriers2016_en.pdf

Extract from the JST News April 2019 edition entitled "Effective Use of Hydrogen Energy with the Power of Formic Acid"

Hydrogen Embrittlement

Hydrogen embrittlement is a phenomenon that occurs when hydrogen atoms are absorbed by a metal. This reduces the ductility of the metal, which reduces its strength. Shimadzu analytical instruments are useful for testing the strength of the materials in pipes and tanks used for the transport and storage of liquid hydrogen and hydrogen gas; for checking the degree of corrosion using X-ray CT scans; and for analysis of the plating process, which may be prone to hydrogen embrittlement.



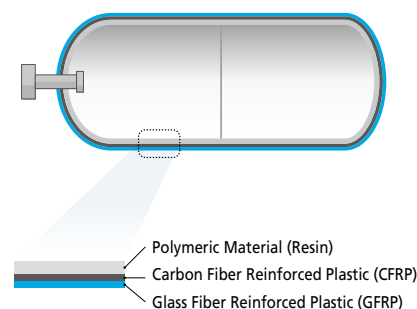
Catalyst Analysis

There are various ways to manufacture hydrogen, including steam reforming and water electrolysis. Regardless of the method, catalysts play an important role in improving efficiency and lowering costs. Accordingly, it is important to evaluate the performance of the catalyst and to check on the degree of deterioration. Catalysts involved in hydrogen manufacturing are often metals such as platinum or palladium. Evaluations can be performed using portable gas concentration measurement instruments. Verifying the degree of deterioration and analyses of the causes of deterioration can be performed using electron probe micro-analyzers and X-ray photoelectron spectrometers.



Hydrogen Tanks

FCVs are equipped with hydrogen tanks. With the high-pressure hydrogen tanks used in vehicles, the higher the hydrogen storage pressure and compressive pressure, the greater the amount of hydrogen that can be stored, which can extend the cruising range of the FCV. For FCV hydrogen tanks, gas tightness, heat resistance, and pressure resistance are important as are reducing the size, weight, and cost. At present, to satisfy the above-mentioned conditions, plastic liners, carbon fiber reinforced plastics, glass fiber reinforced plastics, and other materials are used to create hydrogen tanks. Universal testing machines and thermomechanical analyzers are effective for determining the characteristics of each material. In addition, X-ray CT systems and ultrasonic optical flaw detectors are useful for observing cracks and voids in hydrogen tanks.



Trace Impurity Analysis of Hydrogen Fuel in Fuel Cell Vehicle-Related Fields

Application

If impurities exist in the hydrogen used in fuel cell vehicles, they may poison the catalyst in the cell, reducing catalytic performance. This makes analyzing for impurities in hydrogen a vital task.



Using a barrier discharge ionization detector (BID) with a gas chromatograph enables the high-sensitivity analysis of carbon monoxide in hydrogen and the batch analysis of impurities in the hydrogen.

Measurement Results (Extract)

A Micropacked ST column supports separation of inorganic gasses, including carbon dioxide and lower hydrocarbons, making it suitable for simultaneous analysis of impurities in hydrogen gas. A standard gas was diluted with hydrogen to adjust the component concentrations (other than air components) to about 0.2 ppm, and this gas was analyzed using a Micropacked ST column. The lower limit of detection of carbon monoxide was calculated as 0.078 ppm (S/N=3). The results include detection of the maximum concentration stipulated by ISO 14687-2.

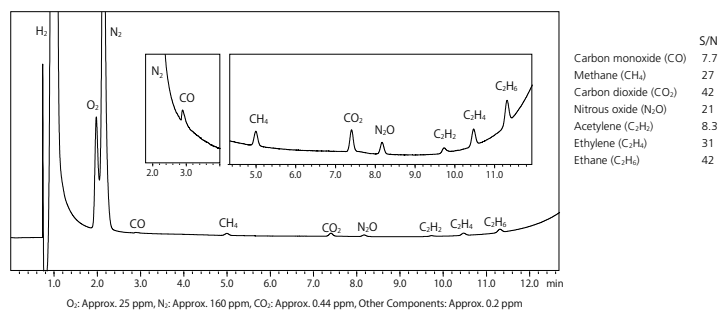
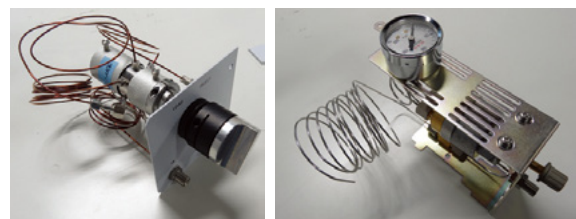


Fig. 1 Chromatogram of Simultaneous Analysis of Impurities in Hydrogen (Micropacked ST Column)

In this analysis, the MGS-2010 gas sampler was used for the introduction of gas into the instrument; the column was connected using the SPLITTER-INJ. Using the MGS-2010 for sample gas injection together with the SPLITTER-INJ unit, it is possible to quantitatively analyze trace-level air components, including Oxygen (O₂), Nitrogen (N₂), etc., with high accuracy.



Valve Unit Manual Flow Controller for Purge

Fig. 2 MGS-2010 Gas Sampler

Gas Chromatograph Nexis GC-2030

This instrument separates each compound in the sample, and then quantifies each component using a detector. The data obtained tells the analyst what compounds are in the sample and in what quantities.

Barrier discharge ionization detector (BID)

Shimadzu's proprietary technology has been adopted for the BID, which incorporates ionization via a new dielectric barrier discharge plasma. It is more sensitive than conventional detectors, is able to detect components that were difficult to detect using FID, TCD and other all-purpose detectors, and delivers long-term stability.

(1) Detectable Compounds

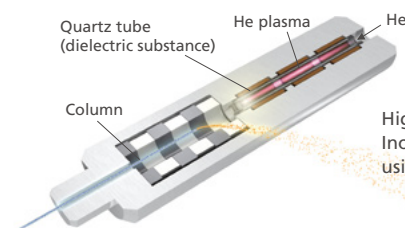
All compounds except He and Ne

(2) Detection Limit

<0.1 ppm (<1.0 pg/sec)

(3) Safety

A plasma with a very low gas temperature is used, which allows the use of hydrogen.



High-Sensitivity Simultaneous Analysis of Inorganic Gases and Light Hydrocarbons using Nexis GC-2030 Dual BID System

Application



Nexis GC-2030 + BID-2030

Product

Analysis of Inorganic Gases and Hydrocarbons by GC-MS

Application 

It is important to measure hydrocarbons as well as N_2 , N_2O and other inorganic gases in hydrogen. If hydrogen fuel contains inorganic gases such as N_2 and N_2O or hydrocarbons, the internal fuel cell mechanism will deteriorate. Measurement of both gases contained in hydrogen is also important.



Inorganic gases and gaseous hydrocarbons can be measured using a porous layer open tubular (PLOT) column.

Measurement Results (Extract)

A total ion current chromatogram is shown in Fig. 3. This column does not separate carbon monoxide from the components in air. Furthermore, at this concentration level, water causes baseline fluctuations.

Extracted ion chromatograms of respective components are shown in Fig. 4. By selecting ions, all 12 components, including those not separated in the total ion current chromatogram, can be analyzed without being affected by water.

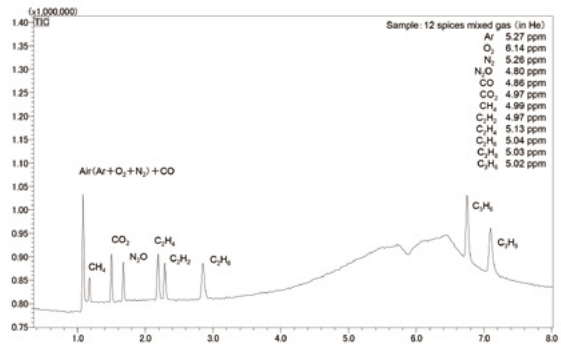


Fig. 3 Total Ion Current Chromatogram

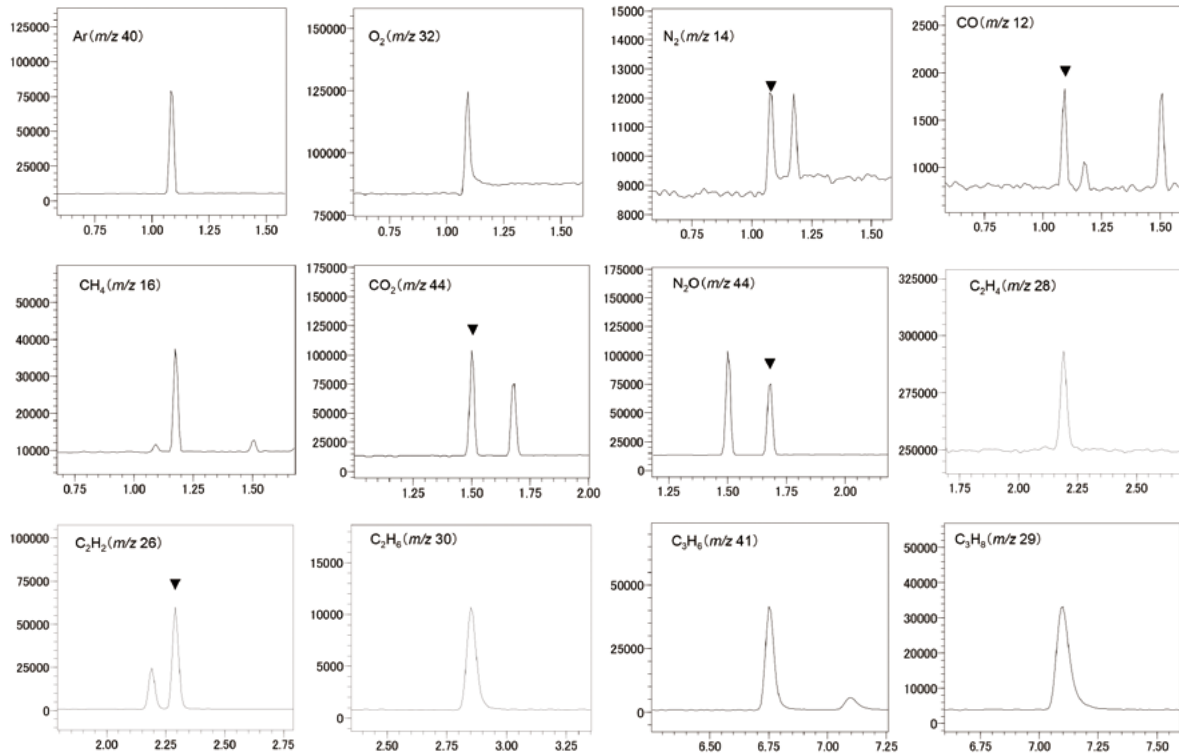


Fig. 4 Mass Chromatograms for Respective Components

High-Resolution Analysis of Carbon Monoxide (CO)

Application 

FTIR is being used for analysis of gases in various industries, such as the gas manufacturing industry where it is used for production management, and for gas monitoring in such fields as chemical manufacturing and semiconductor manufacturing.



- An FTIR with high-resolution can quantify the gas.
- An FTIR can analyze a gas in real time.

Measurement Results (Extract)

Using CO as an example of a low-molecular weight gas, we measured the spectra of CO samples at different concentrations (95 ppm, 191 ppm, 1207 ppm, 2415 ppm) (Fig. 5), and then generated a calibration curve. In this case (Fig. 6), the resolution of 0.25 cm^{-1} was used. For the calibration curve, we used the height of the peak in the vicinity of 2170 cm^{-1} , and primary linear calculations were conducted using the multi-point calibration curve method.

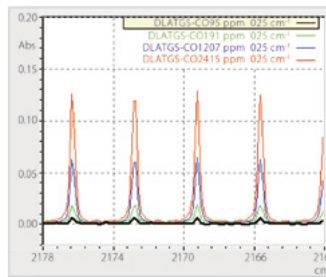


Fig. 5 Overlaid Spectra of CO at Four Concentrations

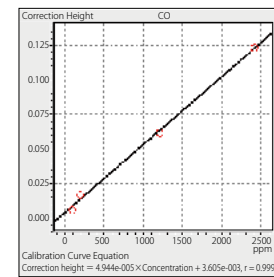


Fig. 6 Calibration Curve of CO Using Four Concentrations

Use of a 10 cm gas cell and a DLATGS detector makes quantitation possible over a wide range of concentrations, from tens to thousands of ppm. The correlation coefficient of $r = 0.999$ for the calibration curve indicated excellent linearity.

To compare spectral differences due to resolution, we measured the infrared spectra of water vapor at resolutions of 0.25 cm^{-1} , 0.5 cm^{-1} and 1 cm^{-1} , respectively (Fig. 7). As can be seen here, the peaks that were not separated at 0.5 cm^{-1} and 1 cm^{-1} were clearly separated when measured with a resolution of 0.25 cm^{-1} . By conducting measurement at high resolution, the spectral peak intensity is noticeably increased, making it easier to distinguish between two peaks that are closely adjacent to one another.

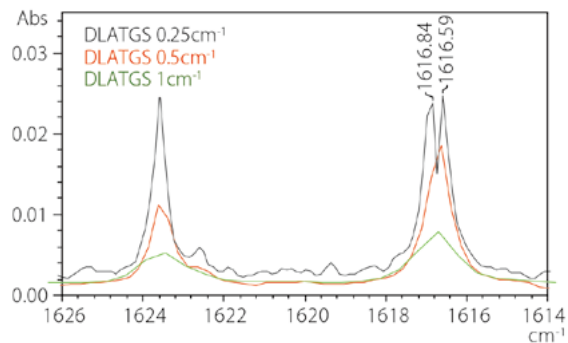


Fig. 7 Overlaid Spectra of Water Vapor Measured at Different Resolutions

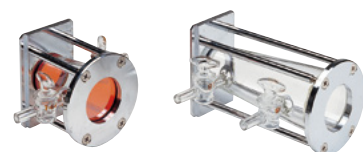
Fourier Transform Infrared Spectrophotometer IRXross

Measurements are performed of the infrared spectrum of the target gas that was injected into the gas cell. Qualitative and quantitative analyses are then performed based on the peak wavenumber and the peak intensity characteristic of the gas.

- The gas injected into the gas cell is measured directly, enabling high-speed analysis. (Approximately 1 minute)
- The instrument is capable of simultaneous multicomponent measurements.
- Pretreatment is not required, so a gas that is changing continuously can be monitored in real time.



Product 



Gas Cell (5 cm, 10 cm)

TOC Evaluation of Ammonia Solution

Application

Ammonia is a focus of interest as a hydrogen carrier. Because high-purity levels are required, measuring for impurities is important.



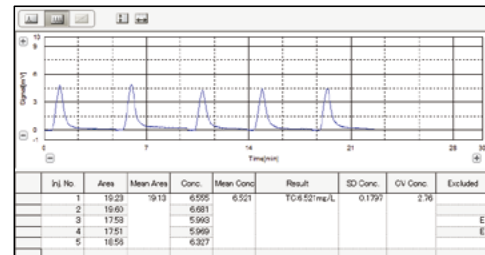
Measurements of organic impurities in ammonia water, which is formed by dissolving ammonia in water, can be performed using TOC analysis. This provides an easy way of monitoring the organic impurities.

Measurement Results (Extract)

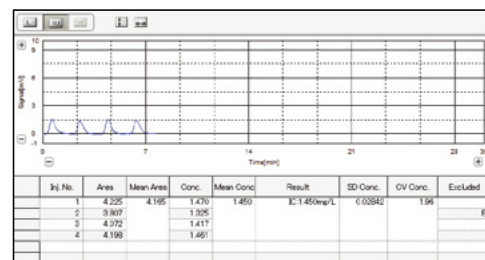
Potassium hydrogen phthalate was added to a 2% ammonia solution to achieve TOC concentrations of 1 mgC/L, 5 mgC/L, and 10 mgC/L, respectively. The total carbon (TC) and inorganic carbon (IC) in the sample were measured, and the TOC was calculated by subtracting the IC from the TC. The system was calibrated for both the TC and IC measurements with standard samples of 0 mgC/L and 20 mgC/L, respectively, and calibration curves were created. The calibration curves were corrected by performing an origin shift to account for the TOC contained in the pure water used in preparing the standard solution. The measurement results for ammonia water are shown in Table 1. An example of the measurement data is shown in Fig. 8. The correlation between the TOC added concentration and the measured concentration is shown in Fig. 9, where the correlation coefficient was 0.9999, indicating good correlation and confirming the accurate measurement of added TOC.

Table 1 Measurement Results of 2 % Ammonia Solution

| Samples | TC [mgC/L] | IC [mgC/L] | TOC [mgC/L] |
|-------------------------------------|------------|------------|-------------|
| 2 % ammonia solution | 0.950 | 0.888 | 0.0624 |
| 2 % ammonia solution + TOC 1 mgC/L | 1.87 | 0.754 | 1.11 |
| 2 % ammonia solution + TOC 5 mgC/L | 6.52 | 1.45 | 5.07 |
| 2 % ammonia solution + TOC 10 mgC/L | 10.3 | 0.481 | 9.83 |



TC Measurement



IC Measurement

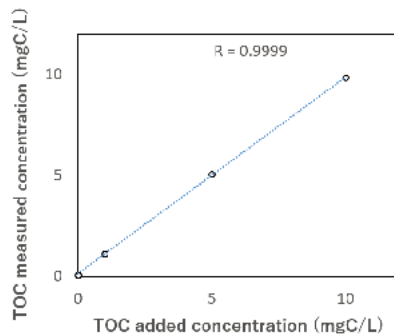


Fig. 9 Correlation between the TOC Added Concentration and the Measured Concentration

Fig. 8 Results of 2 % Ammonia Solution + TOC 5 mgC/L

Total Organic Carbon Analyzer TOC-L

This TOC analyzer adopts the combustion catalytic oxidation method in which the total amount of organic carbon (amount of carbon) is measured by oxidizing the organic substances in the water with carbon dioxide at a high temperature, and then detecting them with an infrared gas analyzer. This is utilized in a variety of fields and applications, including the quality control of tap water.

- While providing an ultra-wide range of 4 µg/L to 30,000 mg/L, these analyzers boast a detection limit of 4 µg/L through coordination with NDIR.
- The combustion catalytic oxidation method makes it possible to efficiently oxidize not only easily-decomposed, low-molecular-weight organic compounds, but also hard-to-decompose insoluble and macromolecular organic compounds.



Product

High-Sensitivity Analysis of Ammonia in Water

Application 

Ammonia is a focus of attention as a hydrogen carrier because of its large energy density per unit volume and how easy it is to store and transport. At the same time, it is known to be toxic and bad smelling, so leakage into the environment is viewed as a problem.



Using a barrier discharge ionization detector (BID) with a gas chromatograph enables a ppm-order analysis of ammonia in water.

Measurement Results (Extract)

Ammonia and methylamine were diluted with water to prepare solutions at 4.8 ppm and 24 ppm, respectively, and the solutions were then measured by GC-BID. The 4.8 ppm and 24 ppm chromatograms are shown in Fig. 10 and the linearity is shown in Fig. 11. Calculating the lower limit of detection ($S/N = 3$) from the 4.8 ppm S/N ratio, the results indicated 1.2 ppm for ammonia and 2.5 ppm for methylamine. Linearity may be sacrificed at low concentrations of components that display adsorption. In this analysis, good linearity was obtained over the range, including at 4.8 ppm and 24 ppm.

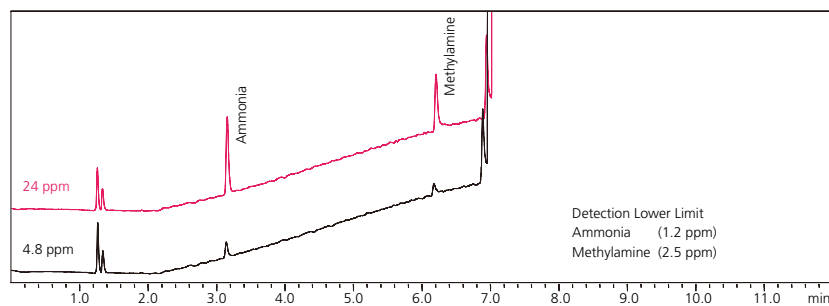


Fig. 10 Chromatograms of 4.8 ppm and 24 ppm Standard Solutions

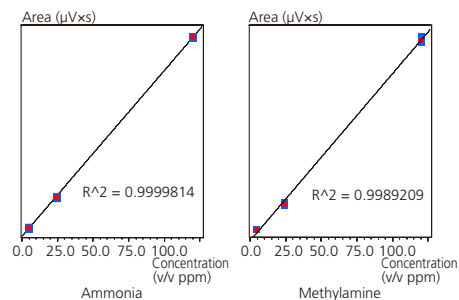


Fig. 11 Linearity of Ammonia and Methylamine (4.8 ppm, 24 ppm)

Gas Chromatograph Nexis GC-2030

This instrument separates each compound in the sample, and then quantifies each component using a detector. The data obtained tells the analyst what compounds are in the sample and in what quantities.

Barrier discharge ionization detector (BID)

Shimadzu's proprietary technology has been adopted for the BID, which incorporates ionization via a new dielectric barrier discharge plasma. It is more sensitive than conventional detectors, is able to detect components that were difficult to detect using FID, TCD and other all-purpose detectors, and delivers long-term stability.



Nexis GC-2030 + BID-2030

Product 

Analysis of Hydrogen in Solution

Application

To use the hydrogen in MCH or ammonia, it must be removed from the hydrogen carrier, so analyses of the hydrogen in the solution and gas are necessary.



Using barrier discharge ionization detectors (BID) enables the high-sensitivity analysis of hydrogen in solution.

Measurement Results (Extract)

With hydrogen and methane as the target analytes, hexanes, toluene and water were used as the dissolving solutions in this experiment. Gas samples at the concentrations of 10, 50, 100, 500, 1,000, and 5,000 ppm (v/v) were prepared by diluting the standard gases of hydrogen and methane with indoor air. Using a 100 µL gas tight syringe, 100 µL of each calibrator was injected into a gas chromatograph (GC) to establish a calibration curve. The chromatogram for hydrogen dissolved in water, hexane, toluene, and other solutions is shown in Fig. 13.

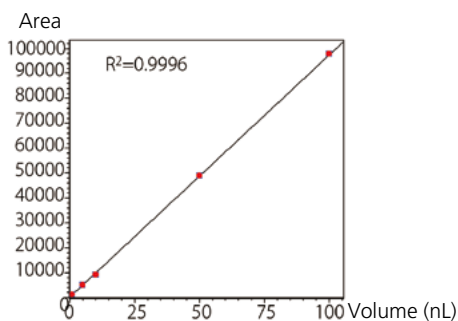


Fig. 12 Calibration Curve of Hydrogen (1, 5, 10, 50, 100 nL)

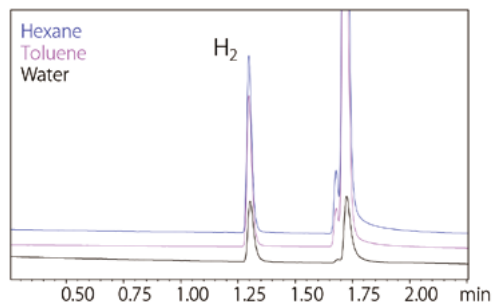


Fig. 13 Chromatogram Overlay of Hydrogen Dissolved in Hexanes, Toluene and Water

Analysis of Hydrogen in Gas

Application

Only certain columns can be used for separation of inorganic gases and light hydrocarbons, and it is sometimes impossible to use a single column to separate all of the target components. The Nexis GC-2030 can be equipped with two BID detectors simultaneously and supports two detectors and columns at the same time.



Inorganic gases and low-level hydrocarbons can be batch analyzed quickly and with high sensitivity by using a dual BID system equipped with two detectors and two columns.

Measurement Results (Extract)

Fig. 14 shows the chromatogram from a batch analysis of five gasses, including hydrogen, other inorganic gases, and low-level hydrocarbons, using a dual BID system.

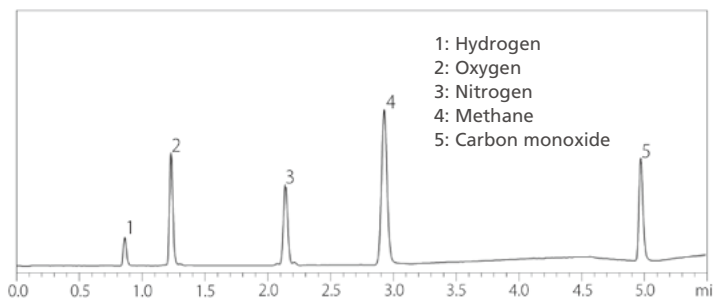


Fig. 14 Chromatogram for 5 ppm Mixed Gas

Analysis of Toluene, Methylcyclohexane (MCH) in Solution

Application 

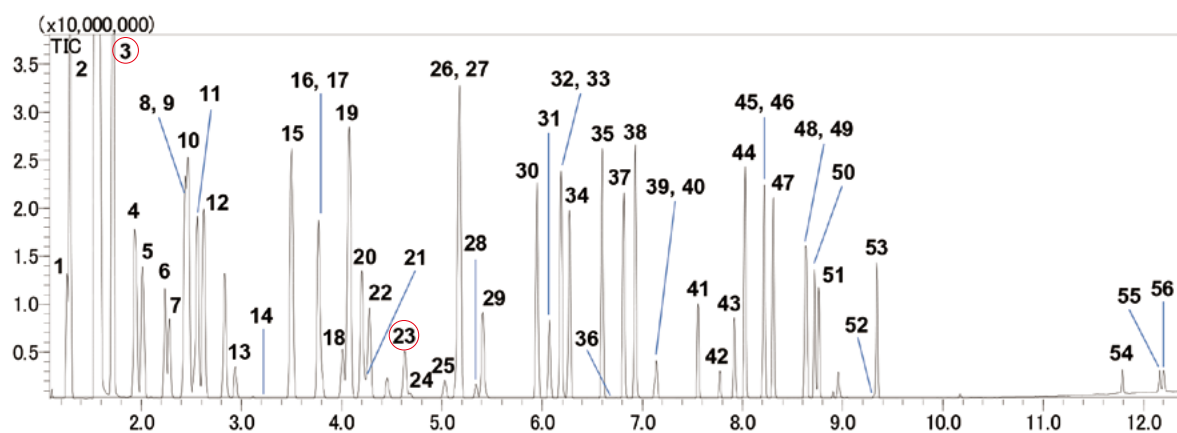
When MCH is used as the hydrogen carrier, toluene is produced when the hydrogen is removed from the MCH, so the MCH and toluene in the solution must be analyzed.



Many organic solvents, including toluene and MCH, in a solution can be analyzed using GC-MS.

Measurement Results (Extract)

Fig. 15 shows the TIC chromatogram from a GC-MS analysis of 56 organic solvents, including toluene and MCH, eluted with carbon disulfide.



1. n-Hexane, 2. Ethyl ether, 3. Methylcyclohexane, 4. Acetone, 5. Methyl acetate, 6. trans-1,2-Dichloroethylene, 7. Tetrahydrofuran, 8. Carbon tetrachloride, 9. 1,1,1-Trichloroethane, 10. Ethyl Acetate, 11. Isopropyl acetate, 12. Methyl ethyl ketone, 13. Dichloromethane, 14. Benzene, 15. n-Propyl acetate, 16. cis-1,2-Dichloroethylene, 17. Trichloroethylene, 18. Methyl isobutyl ketone, 19. Isobutyl acetate, 20. 2-Butanol, 21. Chloroform, 22. Tetrachloroethylene, 23. Toluene, 24. 1,2-Dichloropropane, 25. 1,4-Dioxane, 26. 1,2-Dichloroethane, 27. n-Butyl acetate, 28. Methyl n-butyl ketone, 29. Isobutyl alcohol, 30. Isopentyl acetate, 31. Ethylbenzene, 32. p-Xylene, 33. 1-Butanol, 34. m-Xylene, 35. n-Pentyl acetate, 36. Methyl Cellosolve, 37. o-Xylene, 38. Isopentyl alcohol, 39. Cellosolve, 40. Chlorobenzene, 41. Styrene, 42. Cellosolve acetate, 43. Cyclohexanone, 44. 2-Methylcyclohexanone, 45. N,N-Dimethylformamide, 46. 3-Methylcyclohexanone, 47. 4-Methylcyclohexanone, 48. Butyl Cellosolve, 49. Cyclohexanol, 50. cis-2-Methylcyclohexanol, 51. trans-2-methyl-cyclohexanol, 52. 1,1,2,2-Tetrachloroethane, 53. ortho-Dichlorobenzene, 54. o-Cresol, 55. p-Cresol, 56. m-Cresol

Fig.15 Total Ion Current Chromatogram for 56 Organic Solvents (Stabilwax)

Gas Chromatograph Mass Spectrometer


With this system, the compounds in the sample are separated by component using the gas chromatograph (GC) and these components are ionized in order to analyze their mass. Qualitative information is obtained on the components, enabling a more accurate qualitative analysis than with GC. Any impurities can also be separated. In addition, higher sensitivity enables lower concentration measurements. The pump has a high discharge capacity, so sufficient measurements are possible when using hydrogen as the carrier gas.

Product 

Observation of Corroded Copper Pipe with a Microfocus X-ray CT System

Application

Metal is generally used as the material for pipes and tanks used for the transportation and storage of hydrogen gas and liquid hydrogen. Metal materials become brittle due to hydrogen, so it is necessary to check the degree of deterioration and the decrease in strength of these metals.



Changes in the shape of metal pipes due to corrosion can be observed using a microfocus X-ray CT system.

Measurement Results (Extract)

A copper pipe with an outer diameter of 8.0 mm, a thickness of 0.8 mm, and a length of 30 mm was measured. A 10 g/L aqueous solution of formic acid was used as the organic acid for corrosion. CT scans were performed three times: "before exposure," "after two months exposure," and "after five months exposure".

Fig. 16 shows a three-dimensional data comparison for the outer copper pipe surfaces' corrosion state – before and after exposure. Fig. 16 (a) and 16 (b) show the states after two and five months of exposure. The shape deviation of the outer surface of the copper pipe after exposure to that before exposure is color mapped by superimposing the data before exposure to each data. With a longer exposure period, corrosion progresses. In addition, deep and large dents are observed on the surface.

Fig. 17 is a histogram showing the size of the area for each deviation. The relationship between deviation size and color is unified in Figs. 16 and 17. After two months exposure, we observe an insignificant change; we obtain a large yellow-green area. A significant change is observed after five months of exposure; we observe that the area of blue-green to purple increases with the generation of deep dents, and the histogram spread to the minus side.

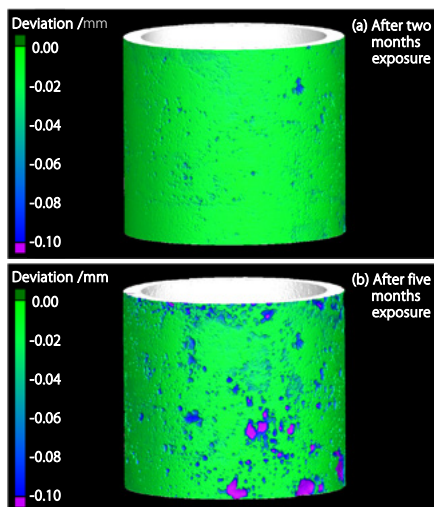


Fig. 16 Example of Shape Analysis: Three-Dimensional Representation of the Corroded Copper Pipe (a) After two months exposure (b) After five months exposure

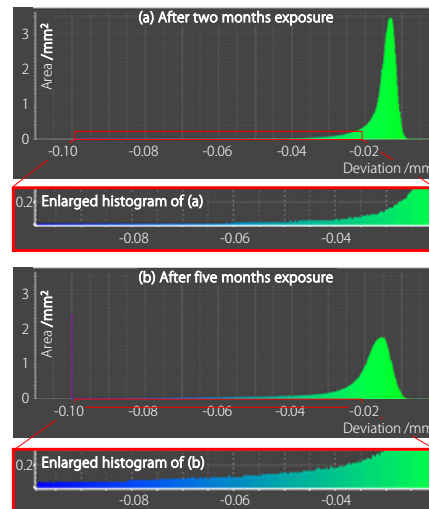


Fig. 17 Example of Shape Analysis: Histogram of the Corroded Copper Pipe (a) After two months exposure (b) After five months exposure

Microfocus X-ray CT System inspeXio SMX-225CT FPD HR Plus

The inspection target is placed between the X-ray generator and the detector. By rotating the target 360 degrees, X-ray transmittance data can be collected from various angles, enabling the acquisition of cross-sectional images and 3D images.

- Speeds up to approximately 50x faster than conventional systems can be achieved.
- The optimal imaging conditions can be easily set by selecting the material, the cross-sectional image resolution, and the contrast.



Product

Accurate Measurements of Micro-Displacements in a Compression Fatigue Test of a Gasket

Application 

Gaskets, which are sealing materials that prevent leakage of gases or liquids and mixing with contaminants, are incorporated at connections in the pipes and tanks used to transport and store hydrogen gas and liquid hydrogen. Evaluating their mechanical characteristics is important.



The fatigue life of a gasket can be evaluated using a Servopulser dynamic and fatigue testing machine.

Measurement Results (Extract)

Displacement gauges were installed at two locations on the left and right sides of the compression plates, and the average value was used to measure the change in the distance between the compression plates (Fig. 18). This allowed for the displacement of the center of the compression plates (the center of the specimen) to be measured even when the compression plates were slanting against the specimen.

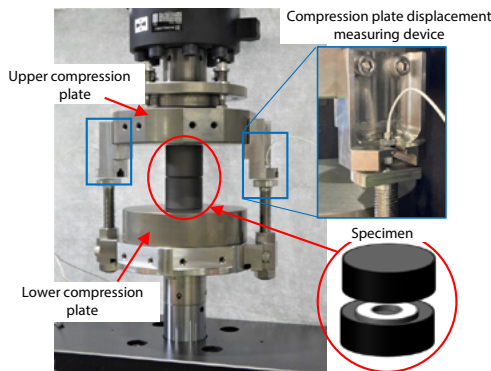


Fig. 18 Test Equipment

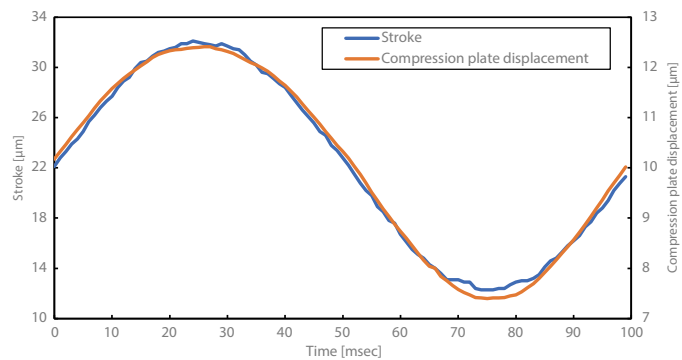


Fig. 19 Displacement Waveform over Time

Fig. 19 shows the stroke and displacement gauge waveforms at cycle 1000, and Table 2 shows the peak values of each waveform. The tests confirmed that at the maximum value, the stroke was about three times larger than the displacement gauge value. This was because the displacement gauge only measured the change in the distance between the compression plates, while the stroke measured the deformation of the jig, etc. Therefore, the measurement points were different. The test demonstrated that the displacement gauge can measure the deformation of a specimen more accurately than the actuator stroke when measuring a displacement of a few μm to tens of μm .

Table 2 Peak Values of Stroke and Displacement Gauge Waveforms

| | Minimum Value [μm] | Maximum Value [μm] |
|--------------------|---------------------------------|---------------------------------|
| Stroke | 12.3 | 32.1 |
| Displacement Gauge | 7.4 | 12.4 |

Servopulser Fatigue and Endurance Testing Machine EHF-E Series

The fatigue life up to the point of breakage can be evaluated by repeatedly loading a sample with stresses and strains.

- Raising/lowering of the crosshead and clamping are easily performed with a single handle.
- The test space is wide, which allows for the attachment of various testing jigs and atmospheric instruments.



Product 

Quantitative Analysis of the Amount of Deposition and Plating Thickness: Multilayer and Irregular Shaped Samples

Application

Surface treatments are applied to prevent the oxidation and deterioration of metals. Hydrogen embrittlement occurs even in the plating process, so optimization of the plating (type and film thickness) is important.



Plating thickness measurements can be performed easily and nondestructively using EDX.

Measurement Results (Extract)

A 3-layer sample comprised as follows: Layer 1: Gold (Au), Layer 2: Nickel (Ni), Layer 3: Copper(Cu) was measured using the thin film FP method. Table 3 shows the results of the quantitative analysis of the amount of deposition. Fig. 21 shows the profiles for each element. The quantitative deposition results indicated values close to the standard value.

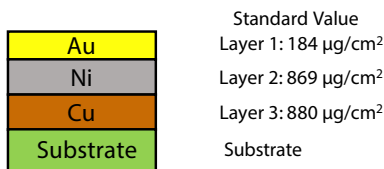


Fig. 20 Layered Plating Configuration of Reference Substance: NMIJ CRM 5208-a

Table 3 Results for the Quantitative Analysis of NMIJ CRM 5208-a [µg/cm²]

| Element | Au | Ni | Cu |
|--------------------|-----|-----|-----|
| Quantitative Value | 176 | 861 | 861 |
| Standard Value | 184 | 869 | 880 |

With the thin film FP method, the result is obtained as the amount of deposition (weight per unit area). This amount of deposition can be converted to plating thickness by dividing by the density (formula shown below). Both the amount of deposition and the plating thickness can be quantitatively determined with Shimadzu EDX.

$$Plating\ thickness\ [nm] = \frac{Plating\ weight\ [\mu g/cm^2]}{Density\ [g/cm^3]} \times 10$$

Table 4 shows the results of converting the deposition values from Table 3 into thin film data. Table 5 shows the results of a simple 10-cycle repeatability test. The improved counting rate increased sensitivity, and the coefficient of variation, which indicates variance, was favorable at less than 1 % max.

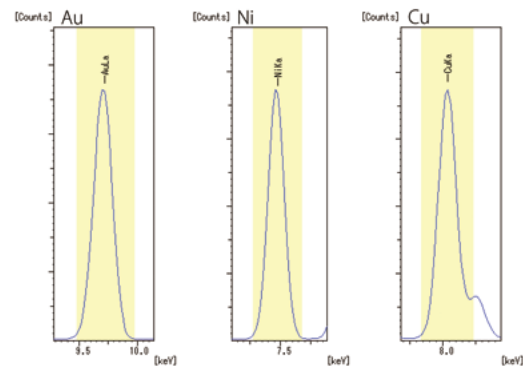


Fig. 21 Overlay of Profiles

Table 4 Results of the Quantitative Analysis of Plating Thickness for NMIJ CRM 5208-a [nm]

| Element | Au | Ni | Cu |
|--------------------|------|------|-----|
| Quantitative Value | 91.1 | 1041 | 937 |

Table 5 Summary of Repeatability Test Results [µg/cm²]

| Element | Au | Ni | Cu |
|------------------------------|------|------|------|
| Average Value | 176 | 862 | 859 |
| Standard Deviation | 0.29 | 0.70 | 4.96 |
| Coefficient of Variation [%] | 0.2 | 0.08 | 0.6 |

Energy Dispersive X-Ray Fluorescence Spectrometer EDX-7200

With an energy dispersive X-ray fluorescence spectrometer, the sample is irradiated with X-rays, and the energy (wavelength) and intensity of fluorescent X-rays emitted are analyzed, enabling an investigation of the types and amounts of elements comprising the sample.

- Samples in various forms, including solids, powders, and liquids, can be analyzed nondestructively.
- With the addition of high-speed circuits, improved algorithms, and increased basic functionality, measurements can be up to 30x faster than with conventional systems.



Product

Evaluation of a Catalyst Used in the Production of Fuel Cell Hydrogen

Application 

Steam reforming introduces a high-temperature catalyst to a mixture of steam and raw materials such as methane or ethanol to produce hydrogen gas. At this point, the concentration changes in the CO and CO₂ produced by the reaction are monitored, enabling an evaluation of the deterioration of the catalyst from changes in the capacity and reaction temperature of the catalyst.



A portable gas analyzer allows for measurement of the concentration of the target gases simply by introducing sample gases and can evaluate the catalytic performance.

Measurement Results (Extract)

Standard methane gas and steam mixed at fixed flowrates were passed through a high-temperature chamber containing a catalyst. Gas discharged from the chamber was cooled to room temperature, liquid generated was drained away, and then gas was introduced to the CGT-7100, which was used to measure concentrations of CO and CO₂ in the exhaust gas sample. The changes in the concentration of the CO and CO₂ over time were continuously monitored. The system is shown in Fig. 22.

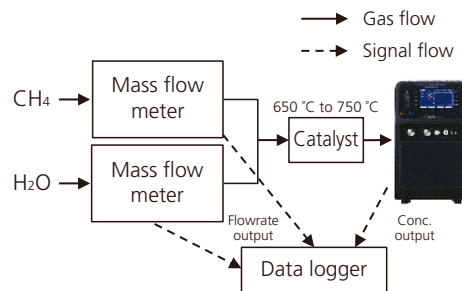


Fig. 22 System Diagram

The measurement results are shown in Fig. 23. The concentrations of CO and CO₂ are heightened by raising the temperature of the catalyst from 650 to 750 °C. It is evident that increasing the temperature of the catalyst increases the reforming capacity.

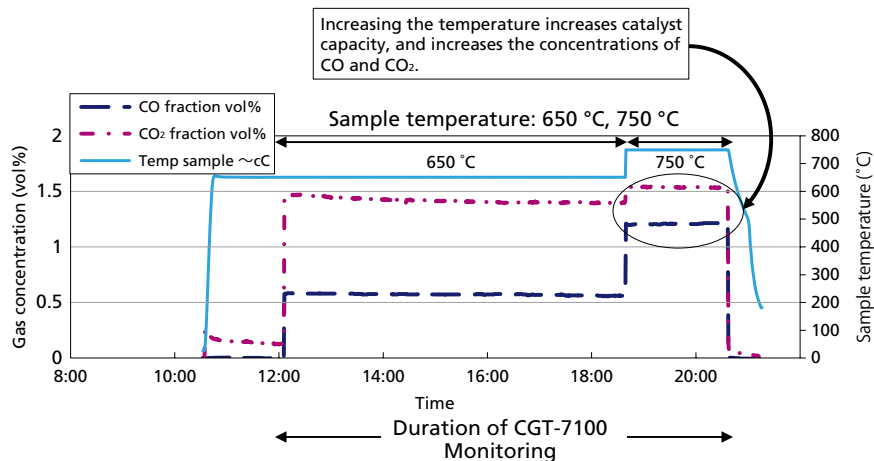


Fig. 23 Measurement Results

Portable Gas Analyzer CGT-7100

The CGT-7100 analyzer measures the concentration of gases in a continuous way using a ratio photometric non-dispersive infrared absorption (NDIR) method.

- All pretreatment parts required for measurement, such as the pump, filter, and electric dehumidifier, are built-in.
- The analyzer can measure two components from CO, CO₂ and CH₄. O₂ measurement is also available as an option.



Product 

Analysis of an Automotive Three-Way Catalyst

Application 

A three-way catalyst (TWC), an automotive catalyst system that was applied practically in the 1970s, uses a combination of three elements to detoxify the harmful components in exhaust gas. Platinum (Pt) and palladium (Pd) oxidize HC (hydrocarbons) to H₂O (water) and CO₂ (carbon dioxide) and oxidize CO (carbon monoxide) to CO₂, while Rh (rhodium) reduces NOx (nitrogen oxides) to N₂ (nitrogen).



Using EPMA, metal scattering and catalyst permeation can be analyzed, enabling investigation of the degree of deterioration of the catalyst.

■ Measurement Results (Extract)

Fig. 24 shows the results of mapping analysis of a Rh-Pd three-way catalyst. It can be understood that trace amounts of the precious metals Rh and Pd are distributed on the upper layer of a two-layer washcoat layer, and promoters such as CeO₂, ZrO₂, La₂O₃, Nd₂O₃, and BaO are composed of different composition ratios in the two (upper and lower) layers.

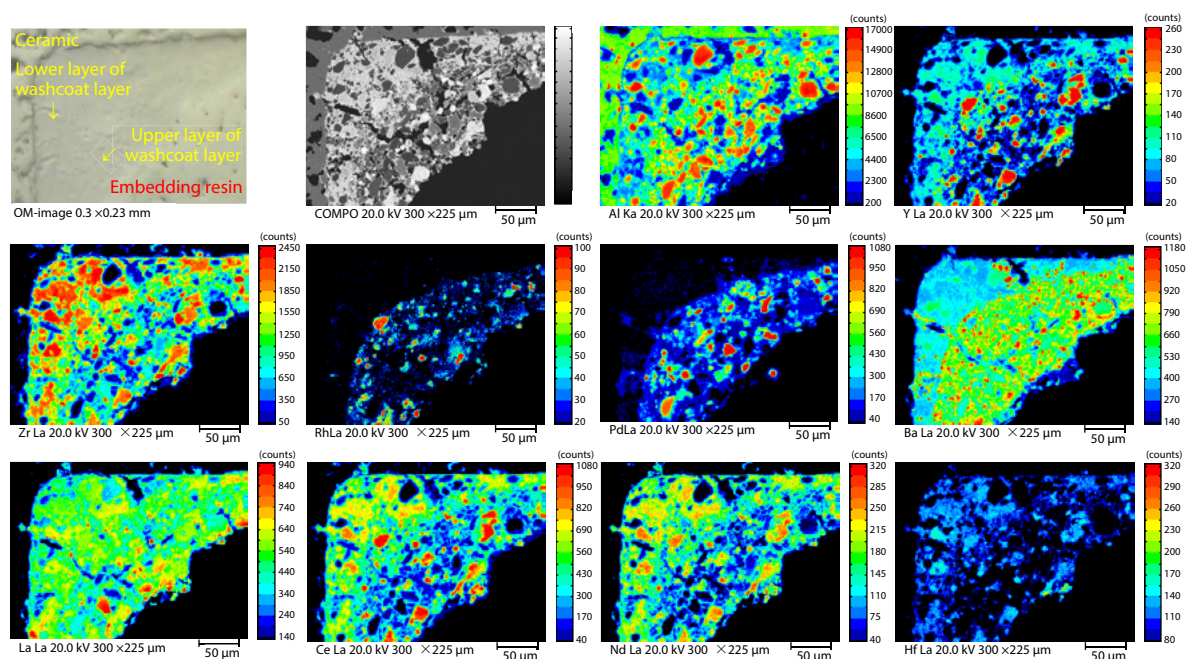


Fig. 24 Mapping Analysis of Rh-Pd Three-Way Catalyst

Electron Probe Microanalyzer EPMA-8050G

With this instrument, the surface of a solid sample is irradiated with an electron beam, enabling analysis of the elements in the sample surface and observation of its morphology.

- Large beam current enabling ultra-high-sensitivity analysis.
- The X-ray take-off angle is high, and the spatial resolution is very high.
- All operations can be performed with just a mouse.

Product 

Analysis of an MEA (Membrane/Electrode Assembly) by EPMA

Application 

Electrochemical devices in which electrode catalyst layers are bonded on a solid polymer electrolyte membrane, which is a hydrogen ion conductor, are called membrane electrode assemblies (MEA), and are used in diverse applications, including fuel cells, technologies for water electrolysis hydrogen production technologies, and dehumidifying cells. Catalytic cohesion is one example of MEA performance deterioration, so it is important to assess the distribution of elements in the vicinity of the MEA surface.



Using EPMA, it is possible to perform a comparative evaluation of a new MEA before use and a deteriorated MEA.

Measurement Results (Extract)

Fig. 25 shows a structural diagram of an MEA. The surface of the anodic side is covered with an electrode catalyst layer and is coated with a mixture of a Pt catalyst and an ionomer (solid polymer electrolyte membrane). The solid polymer electrolyte membrane is positioned under this coating, and a lattice-shaped (+) electrode grid is embedded in the membrane.

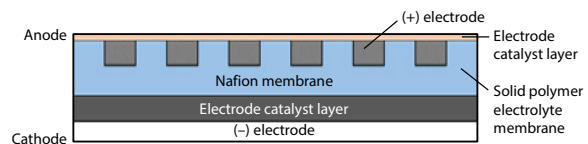


Fig. 25 Structural Diagram of MEA

Fig. 26 shows the results of a mapping analysis of the surface of the anodic side of this MEA. The left side shows the results for a new product, and the right shows a product with deteriorated performance. A relative comparison of intensity values is possible by measuring the new product and deteriorated product under the same conditions. Looking at the distribution of Pt in the deteriorated product, the intensity has decreased, while the intensity of S, which is an ionomer component (sulfonic acid), has increased. Because C and O display particularly high intensities in the electrode grid part, and conversely, the intensity of F has decreased in this grid part, the elevated levels of C and O are thought to show the effects of adhering contamination and surface oxidation.

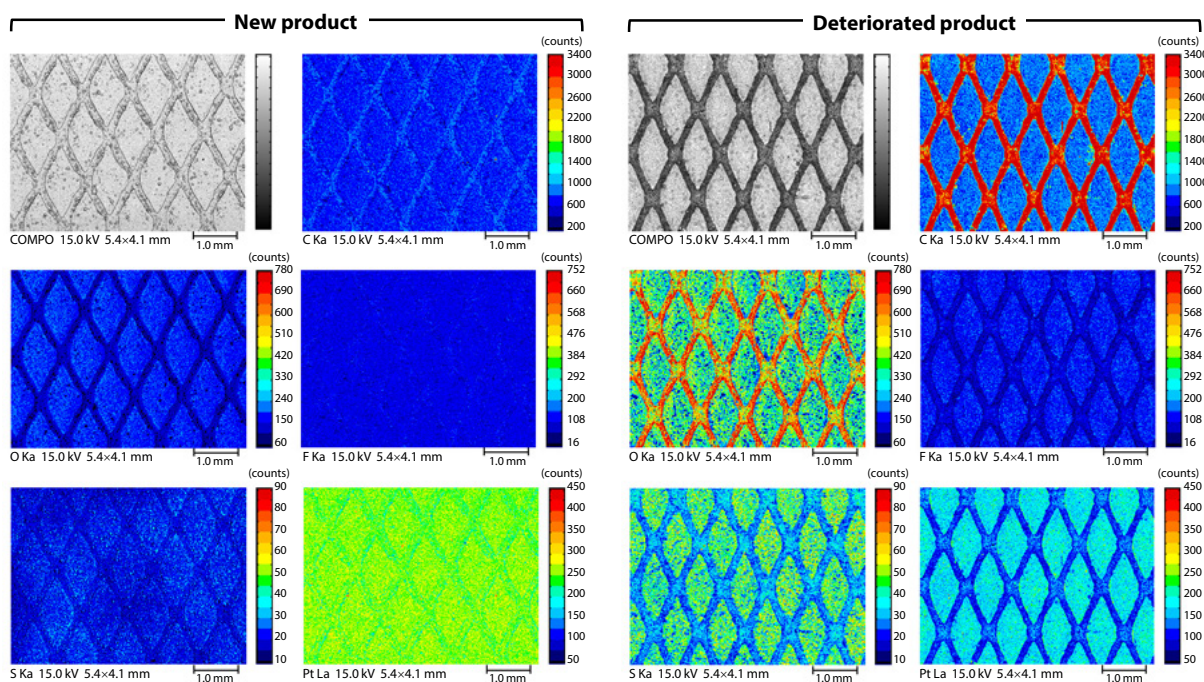


Fig. 26 Mapping Analysis of MEA Surface (Left: New product, Right: Deteriorated product)

Analysis of an MEA (Membrane/Electrode Assembly) by XPS

An MEA is an electrochemical device in which an electrode catalyst is bonded to a solid polymer electrolyte membrane. MEAs are utilized in fuel cells and water electrolysis hydrogen production technologies. It is necessary to increase the chemical stability of the electrolyte membrane to improve the performance and operating life of MEAs. For this reason, it is important to analyze the layered structure and deterioration in proximity to the surface of MEAs.



Using an X-ray photoelectron spectrometer (XPS), information about the chemical state of the surface of a degraded MEA can be obtained.

Measurement Results (Extract)

Two MEAs were studied: a new, unused one (sample A), and a degraded one with reduced performance due to long-term use in a particular environment (sample B). Fig. 27 shows the peak fitting results for the Pt 4f spectrum. Pt(0), PtO, Pt(OH)₂, and PtO₂ were present in the electrode catalyst layers of samples A and B. However, there were clear differences in the ratio of components between each sample. In sample B, while the ratio of Pt(0) was reduced, it can be confirmed that the amount of PtO₂ had increased. These results suggest that the platinum in the surface layer of the anode electrode catalyst in sample B is oxidized.

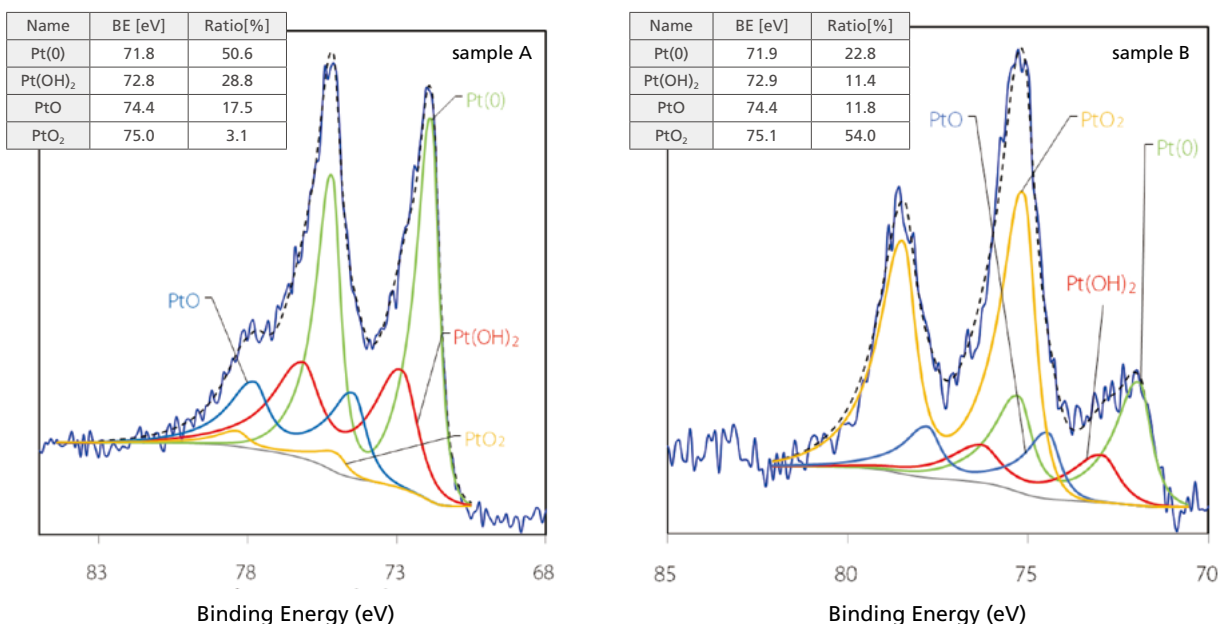
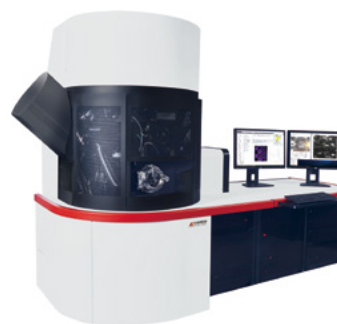


Fig. 27 Pt 4f Peak Fitting Results for Samples A (left) and B (right)

Imaging X-ray Photoelectron Spectrometer AXIS Supra⁺

In addition to a qualitative and quantitative analysis of elements, a chemical state analysis can be performed. AXIS Supra⁺ provides unrivalled large area spectroscopic performance, and fast, high spatial resolution XPS imaging capability.

- Fully automated sample handling
- Multi-technique capability - Compatible with AES, REELS, UPS, ISS and other analytical techniques



Product

Observation of Carbon Fiber Reinforced Thermoplastic Resin with an X-ray CT System

Application 

Carbon fiber reinforced plastic (CFRP) is used for the hydrogen tanks built into fuel cell vehicles. CFRP has better mechanical properties than conventional plastic materials, but voids and cracks in the interior produced during the manufacturing process can lead to product malfunctions. To stabilize the quality of the CFRP, it is important to investigate whether there are any voids or cracks within the resin, and whether the fiber orientation is as designed.



Using an X-ray CT system, it is possible to observe voids and cracks nondestructively. Additionally, graphs can be displayed in which the color corresponds to the angle of deviation of the fibers.

Measurement Results (Extract)

Fig. 28 shows the external appearance of the carbon fiber reinforced thermoplastic (CFRTP) sample scanned in this experiment. This is a multilayered laminated material with overall dimensions of 30 mm × 3 mm × 1 mm. Fig. 29 shows an MPR (Multi Planar Reconstruction) screen, in which cross sections seen from multiple angles are displayed on the same screen after a portion of the sample has been scanned by a CT system. The numbers at the upper left of each screen and the lines drawn in the screens show the location of each cross section in the sample. In the cross-sectional images, higher density areas are whiter as the density increases, while lower density areas are blacker, making it possible to observe voids, cracks, resin, and carbon fibers from the screen. As shown in Fig. 30, the CT data are displayed on screens showing 3-dimensional representations for easier understanding of the structure of the scanned sample. Here, the laminated structure formed by the orthogonally-arranged layers of carbon fibers and a crack near the surface can be observed.

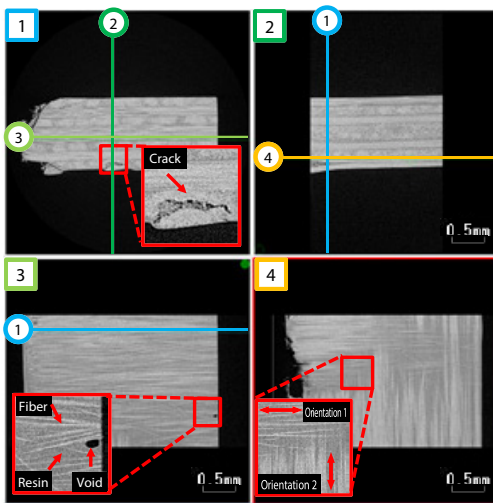


Fig. 29 MPR Screen Showing Cross-Sectional Images of CFRTP



Fig. 28 External Appearance of CFRTP Sample

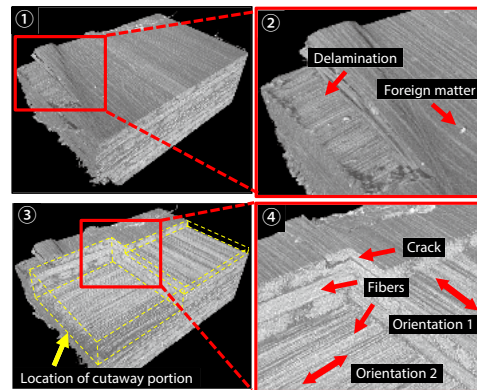


Fig. 30 Screens Showing 3D Representations of CFRTP

Fig. 31 is a screen showing the result of an analysis of the fiber orientation. The standard orientation is set to 0° in the data, and the fibers in the CFRTP are colored corresponding to their deviation angles. In the histogram (Fig. 32), the horizontal axis shows the angle of deviation from the standard for the fibers, and the vertical axis shows the frequency of each angle of deviation. These results show that many of the fibers are oriented at 90° to the standard orientation.

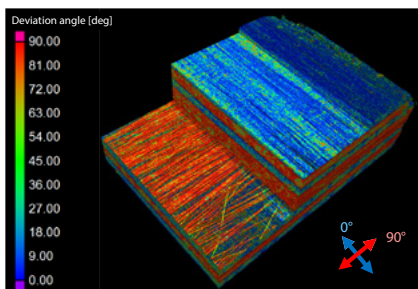


Fig. 31 Screen Showing 3D Representation of CFRTP: Fiber Orientation Analysis

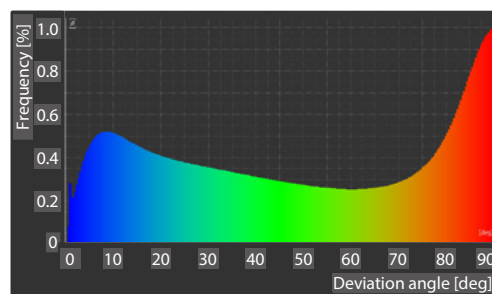



Fig. 32 Histogram Showing Fiber Orientation Angles of CFRTP

Verification and Validation of Uniaxial Tensile Test Simulation Results of Composites

Application 

Unlike metal materials, composite materials have a complex internal structure and display complex fracture behavior, depending on the principal axis of applied stress, making it difficult to establish highly accurate structural analysis models. Improved reproducibility of CAE analysis is expected to increase efficiency and reduce costs in development work, and to improve the reliability of the designs of both complex and large-scale structures, which is difficult to assess by actual measurement.



- The structural information obtained by the X-ray CT system can be reflected in the structural analysis simulation models.
- Using a universal testing machine and a non-contact extensometer, it is possible to acquire image data synchronized to the load.

Flow of Analysis

For the analysis, virtual material testing (hereinafter, numerical material testing or NMT) was conducted for the default structural data (Model 1) generated automatically by Multiscale.Sim™ and for the structural data (Model 2) generated by using data acquired by a microfocus X-ray CT system, as described below.

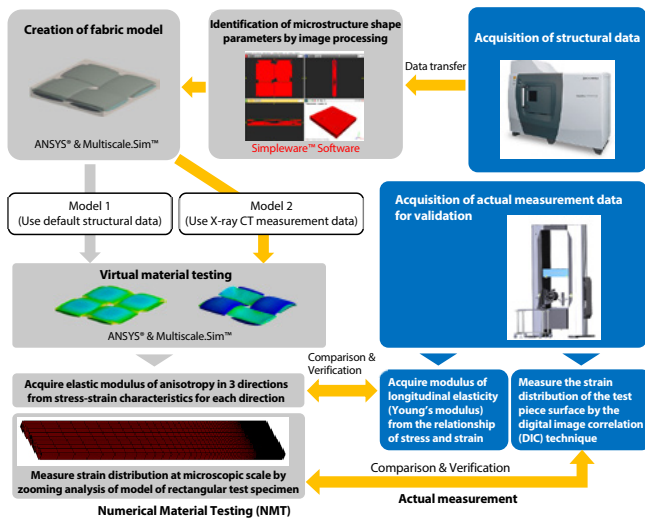


Fig. 33 Flow of Analysis

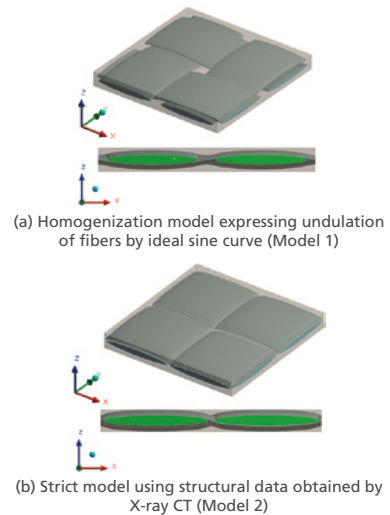


Fig. 34 Two Analysis Models Examined

In NMT, the two models (Model 1 and Model 2) shown in Fig. 34 were used. For Model 1, the default structural data registered in the software was used. The cross-sectional shape is uniform for fiber bundles, and the fiber bundle shape displays sinewave-like undulations. On the other hand, with model 2, the cross-sectional shape of the fiber bundles is not uniform, and the undulations deviate from the sinewave form and follow the cross-sectional shape of the fibers.

Table 6 Comparison of Modulus of Longitudinal Elasticity Obtained by Homogenization Analysis and Actual Measurement Results

| Material | Homogenization analysis (Model 1) | | Homogenization analysis (Model 2) | | Uniaxial tensile test (Actual measurement) |
|----------|--|---|--|---|--|
| | Modulus of longitudinal elasticity (GPa) | Rate of agreement with actual measurement (%) | Modulus of longitudinal elasticity (GPa) | Rate of agreement with actual measurement (%) | Modulus of longitudinal elasticity (GPa) |
| CFRP | 32.555 | 58.7 | 51.751 | 93.3 | 55.46 |

Table 6 summarizes the results of comparison of the elastic modulus identified by NMT and the elastic modulus obtained in the uniaxial tensile test (actual measurement). Fig. 35 shows the nominal stress-nominal strain curves obtained from the uniaxial tensile test (actual measurement) and NMT. The elastic modulus in the direction of uniaxial tension was 55.46 [GPa] in the uniaxial tensile test (actual measurement), but was 32.56 [GPa] with Model 1, showing a large error in the simulation result. In contrast, the modulus of longitudinal elasticity with Model 2 was 51.75 [GPa], which was close to the measured value. Relative error was reduced by reflecting the structural data obtained with the microfocus X-ray CT system in the analysis model.

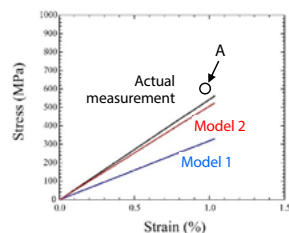


Fig. 35 Comparison of Results of Nominal Stress-Nominal Strain Curves in Actual Measurement and NMT

Example of Non-Destructive Inspection Using an Ultrasonic Optical Flow Detector

Plastic liners, carbon fiber reinforced plastics, glass fiber reinforced plastics, and other materials are used to create hydrogen tanks, and the junctions between these materials must be inspected.



With its light imaging technique, which combines an ultrasonic oscillator with a stroboscope, defects near the surface of a material, including peeling of the bonding and adhesive surfaces of heterogeneous materials, as well as paint, thermal sprays, and coatings can be inspected easily and non-destructively.

Inspection of Adhesive Surface Delamination between CFRP and Stainless Steel

[Sample provided by: Nagoya Municipal Industrial Research Institute]

Movie

Artificially created delamination is detected non-destructively. Further, with X-ray fluoroscopy, unconfirmed delamination (bottom right) is detected.

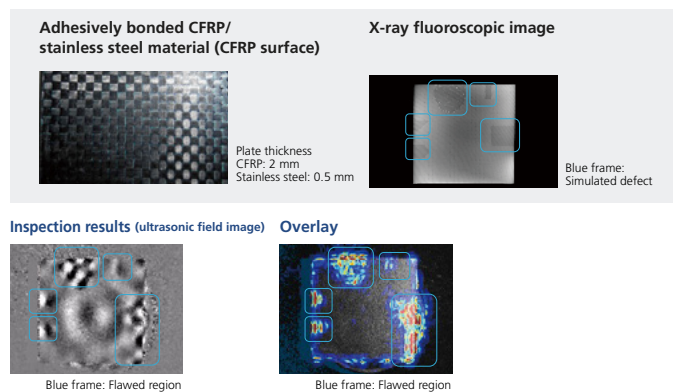
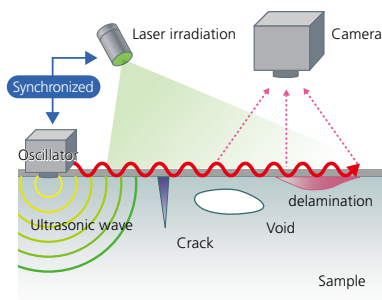


Fig. 36 Inspection of Adhesive Surface Delamination between CFRP and Stainless Steel

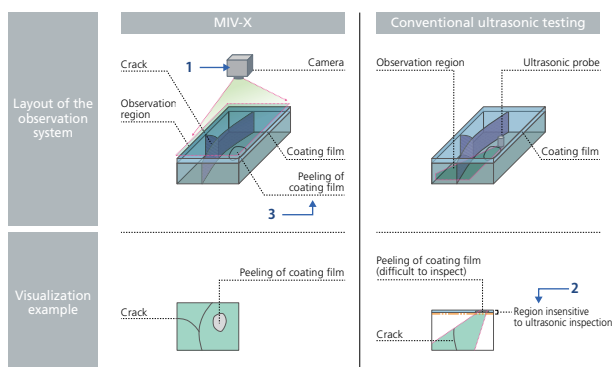
Ultrasonic Optical Flow Detector MIV-X

With ultrasonic optical flow detection technology the displacement of the surface is detected optically, and the propagation of the ultrasonic wave on the surface is observed.

- The sample is loaded by continuous ultrasonic vibrations.
- Microscopic out-of-plane displacement of the surface due to propagation of the ultrasonic wave is visualized optically using laser irradiation and a camera.
- Defects are detected by observing disturbances in the propagation of the ultrasonic wave.




The MIV-X Ultrasonic Optical Flow Detector assists with regions where ultrasonic testing (UT) is difficult.




Product

Measurement of Expansion Coefficient of Polymer Materials Using TMA

Application 

The hydrogen tanks that store liquid hydrogen are exposed to very low temperatures, so it is important to evaluate their thermal expansion/shrinkage and expansion coefficient in order to prevent deterioration and damage due to thermal changes.



benefits

A thermomechanical analyzer can evaluate the linear expansion coefficient of materials with various shapes, and can even perform measurements starting from temperatures as low as -150 °C.

■ Measurement Results (Extract)

Several types of differently shaped high-polymer materials were measured, and their thermal expansion/shrinkage and linear expansion coefficients were evaluated. Firstly, the expansion coefficient of a polyethylene sheet approximately 0.5 mm thick was measured. Fig. 37 shows that the sample expands linearly as the temperature rises. The coefficient of thermal expansion of the sample obtained over the temperature range of 40 to 80 °C was $215.41 \times 10^{-6}/K$. In expansion mode, the expansion coefficient can even be measured for the thickness direction of sheet-like samples with a thickness of less than 1 mm.

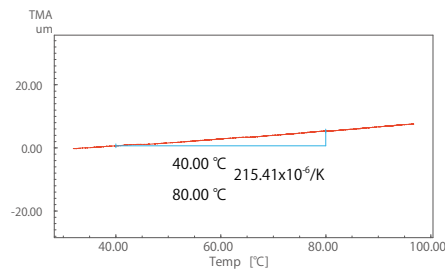


Fig. 37 Polyethylene Sheet Expansion Measurement Results

Next, two separator films for a lithium-ion battery were measured. A sample set in the chucks is shown in Fig. 38, and the measurement results are shown in Fig. 39. The separator film in a lithium-ion battery has a significant impact on the performance and safety of the battery. Comparing the two types of film from the point of view of preventing short circuits, the temperature when shrinkage occurs is higher in Film A than Film B, so Film A is safer in terms of heat resistance. However, the amount of shrinkage is smaller for Film B than Film A, so Film B is actually safer for a device.



Fig. 38 View of the Sample and Chucks

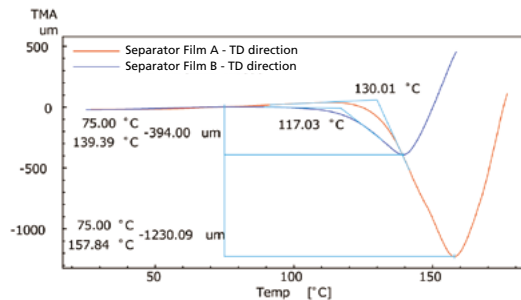
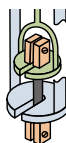


Fig. 39 Measurement Results of the TD Direction for Two Separator Films

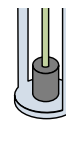
Thermomechanical Analyzer TMA-60

A thermomechanical analyzer (TMA) changes the sample temperature as programmed, and measures changes in the shape of the sample while applying a certain pressure to it during the process. Three types of measurement: tensile, expansion, and needle penetration, can be performed starting at -150 °C.

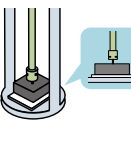
Tension Measurement



Expansion Measurement



Penetration Measurement





Product 

DCB Tests of CFRP

Application 

CFRP laminates are not impact-resistant, and damages such as delamination can occur on impact. Therefore damage-tolerant designs, which take into consideration the effect of internal damage on the strength of the material, are incorporated in design and product development. In order to implement damage-tolerant designs, it is necessary to determine the resistance to delamination growth, so fracture toughness tests are performed.



- It is possible to measure the interlaminar fracture toughness, which is necessary for designing CFRP.
- The delamination length can be observed after testing by video recording the delamination growth using TRViewX.

Measurement Results (Extract)

In these tests, a scale for confirming the delamination growth was marked on one side of the test specimen, while on the other side a crack gauge was installed for confirming the delamination length (Fig. 40). In these tests, the extent of delamination growth was monitored up to a length of 50 mm from the tip of the initial delamination. Using TRViewX to save the video made it possible to perform the calculations while reviewing the video synchronized with the results after the tests. In the specimens tested, delamination growth was initially unstable, with the force dropping suddenly at point A. Subsequent delamination growth was stable, with fracture occurring at 45 to 50 mm (Fig. 41). With the TRViewX image, it was possible to check the propagation of cracks all the way to the end (Fig. 42).

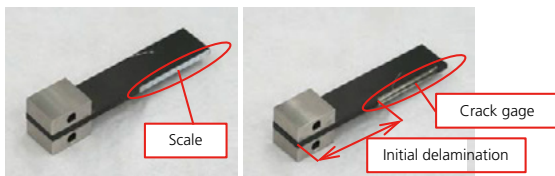


Fig. 40 Test Specimen (Left: Scale Side, Right: Crack Gauge Side)

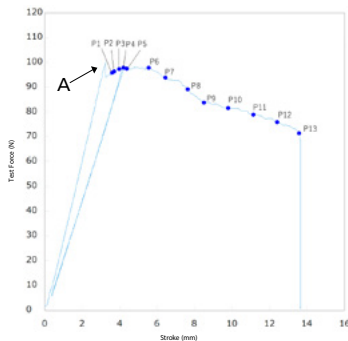


Fig. 41 Test Results

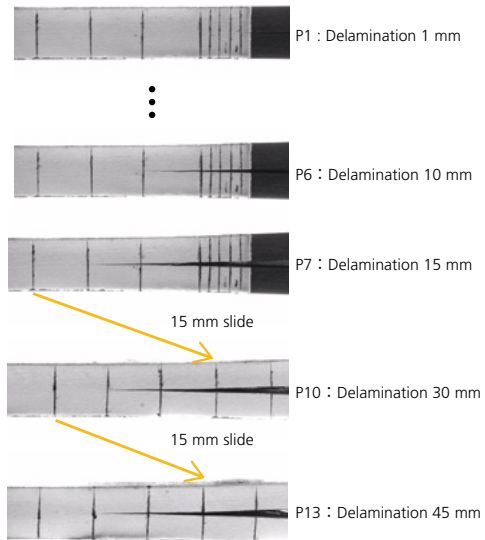


Fig. 42 Test Results and Linked TRViewX Images

Precision Universal Tester AGX-V2 Series

Fracture toughness tests can be performed to check the impact of interlaminar peeling and damage in CFRP laminate materials.



Product 

Non-Contact Digital Video Extensometer TRViewX

While film elongation measurements are difficult with a contact extensometer, the TRViewX non-contact digital video extensometer can perform accurate elongation measurements across a wide elongation range without affecting the sample.



Product 



Shimadzu Corporation

www.shimadzu.com/an/

For Research Use Only. Not for use in diagnostic procedures.

This publication may contain references to products that are not available in your country. Please contact us to check the availability of these products in your country.

Company names, products/service names and logos used in this publication are trademarks and trade names of Shimadzu Corporation, its subsidiaries or its affiliates, whether or not they are used with trademark symbol "TM" or "®".

Third-party trademarks and trade names may be used in this publication to refer to either the entities or their products/services, whether or not they are used with trademark symbol "TM" or "®".

Shimadzu disclaims any proprietary interest in trademarks and trade names other than its own.

The contents of this publication are provided to you "as is" without warranty of any kind, and are subject to change without notice. Shimadzu does not assume any responsibility or liability for any damage, whether direct or indirect, relating to the use of this publication.